

Article

Influence of Sawdust Particle Sizes on the Physico-Mechanical Properties of Unfired Clay Blocks

Nusrat Jannat ^{1,*}, Rafal Latif Al-Mufti ¹, Aseel Hussien ², Badr Abdullah ¹  and Alison Cotgrave ¹

¹ School of Civil Engineering & Built Environment, Liverpool John Moores University, Byrom Street, Liverpool L3 3AF, UK; R.A.LatifAlMufti@ljmu.ac.uk (R.L.A.-M.); B.M.Abdullah@ljmu.ac.uk (B.A.); A.J.Cotgrave@ljmu.ac.uk (A.C.)

² Department of Architectural Engineering, University of Sharjah, Sharjah 341246, United Arab Emirates; ahussien@sharjah.ac.ae

* Correspondence: N.Jannat@2019.ljmu.ac.uk

Abstract: Sawdust, which is a waste/by-product of the wood/timber industry, can be utilised as a valuable raw material in building material production due to its abundance and low cost. However, the application of sawdust in the manufacture of unfired clay blocks has received little investigation. Furthermore, the impact of different sawdust particle sizes on the properties of unfired clay blocks has not been studied. Therefore, this study screened sawdust at three different particle sizes: SP-a ($212\ \mu\text{m} < x < 300\ \mu\text{m}$), SP-b ($425\ \mu\text{m} < x < 600\ \mu\text{m}$) and SP-c ($1.18\ \text{mm} < x < 2.00\ \text{mm}$), to examine their effects on the physical and mechanical properties of unfired clay blocks. The density, linear shrinkage, capillary water absorption and flexural and compressive strengths were among the tests performed. Different sawdust percentages, i.e., 2.5%, 5%, 7.5% and 10% of the total weight of the clay, were considered. The tests results show that when sawdust was added to the mixture, the density of the samples reduced for all particle sizes. However, the linear shrinkage increased in SP-a samples but decreased in the other two particle size samples as the sawdust percentage increased from 2.5% to 10%. On the other hand, the capillary water absorption coefficient increased while the strength decreased with increasing sawdust content for all three groups. The highest compressive strength (CS) and flexural strength (FS) were achieved at 2.5% of sawdust content. Furthermore, it was observed that SP-b (CS—4.74 MPa, FS—2.00 MPa) samples showed the highest strength followed by SP-a (CS—4.09 MPa, FS—1.69 MPa) and SP-c (CS—3.90 MPa, FS—1.63 MPa) samples. Consequently, good-quality unfired clay blocks can be manufactured using sawdust up to 2.5% with particle sizes ranging between 600 and 425 μm .



Citation: Jannat, N.; Latif Al-Mufti, R.; Hussien, A.; Abdullah, B.; Cotgrave, A. Influence of Sawdust Particle Sizes on the Physico-Mechanical Properties of Unfired Clay Blocks. *Designs* **2021**, *5*, 57. <https://doi.org/10.3390/designs5030057>

Academic Editor: Tiago Ribeiro

Received: 14 August 2021

Accepted: 13 September 2021

Published: 14 September 2021

Publisher's Note: MDPI stays neutral with regard to jurisdictional claims in published maps and institutional affiliations.



Copyright: © 2021 by the authors. Licensee MDPI, Basel, Switzerland. This article is an open access article distributed under the terms and conditions of the Creative Commons Attribution (CC BY) license (<https://creativecommons.org/licenses/by/4.0/>).

Keywords: wood by-products; sawdust; particle size; clay blocks; unfired

1. Introduction

Currently, there is a great interest in adopting alternative sustainable building materials in the construction industry, and researchers have been engaged in manufacturing novel building materials utilising different wastes/by-products. In this context, the social, economic and environmental sustainability of earthen building materials enhanced with agricultural wastes/by-products has become apparent. These materials require less energy to process and offer good technical characteristics. Sawdust is considered as a waste material which is a by-product of the wood/timber industry and produced by the cutting, sawing or grinding of timber. Every year, sawmills produce huge volumes of sawdust [1,2] (Figure 1). According to one report, the average annual growth rate of the global wood harvest was 0.20% between 1990 and 2015 [3], and the FAO estimates a 55% increase in the potential industrial roundwood supply by 2030 [4]. As a result, the timber industry is becoming more concerned about the cost-effective disposal of sawdust as the bulk of it is burned off, polluting the environment [5–7]. Sawdust, on the other hand, can be used as a valuable raw material in a variety of industries due to its abundance

and low cost. Sawdust is mainly composed of cellulose, hemicelluloses, lignin and small amounts (5–10%) of extraneous materials [8–10]. It is most commonly used in the energy, agriculture and manufacturing industries [5]. However, little research has been performed on the application of sawdust in the production of building materials [11]. Sawdust-based insulation materials [12], particleboard [13–18], cement concrete bricks [19,20], fired clay bricks [21–26] and unfired bricks [27–35] are some of the developed building materials. Ouattara et al. [30] showed that with the incorporation of sawdust (0–25%), the dry density of compressed clay bricks decreased, while the strength increased, for a 15–20% sawdust content. Similarly, Demir [27] utilised 2.5–10 wt% of sawdust in unfired bricks and found that the compressive strength gradually improved with the addition of sawdust. Fadele and Ata [31] used sawdust lignin additives and cement (4, 8 and 12% by mass) to investigate the water absorption characteristics of compressed earth blocks, where the samples with sawdust additives performed better than the samples with cement. The thermal performance of sawdust (2–10 wt%)-stabilised unfired bricks was assessed by Charai et al. [34], and the results revealed that the addition of sawdust reduced both the density and thermal conductivity of the brick samples. Ganga et al. [29] evaluated the mechanical and acoustic properties of clay bricks with different percentages of cement, sawdust and mahogany shavings. It was found that the addition of sawdust or mahogany shavings did not improve the compressive strength of the samples. Jokhio et al. [32] measured the compressive and flexural strengths of adobe bricks by partially replacing sand with sawdust (0–40%). The findings revealed that about 20% of the sand substitute provided the highest compressive strength, while the flexural strength decreased gradually as sawdust was added to the mixture. In another study, Vilane [28] investigated the compressive strength of adobe blocks incorporating sawdust (0–20%) and recommended the optimal percentage to be 15%. De Castrillo et al. [35] reproduced traditional adobe bricks using straw and sawdust fibres (30–70% by volume). For both fibre types, increasing the fibre content resulted in decreasing the bulk density, thermal conductivity and flexural and compressive strengths of the adobes. Moreover, in contrast to straw adobes, sawdust adobes showed a general rise in capillary absorption as the fibre percentage increased.

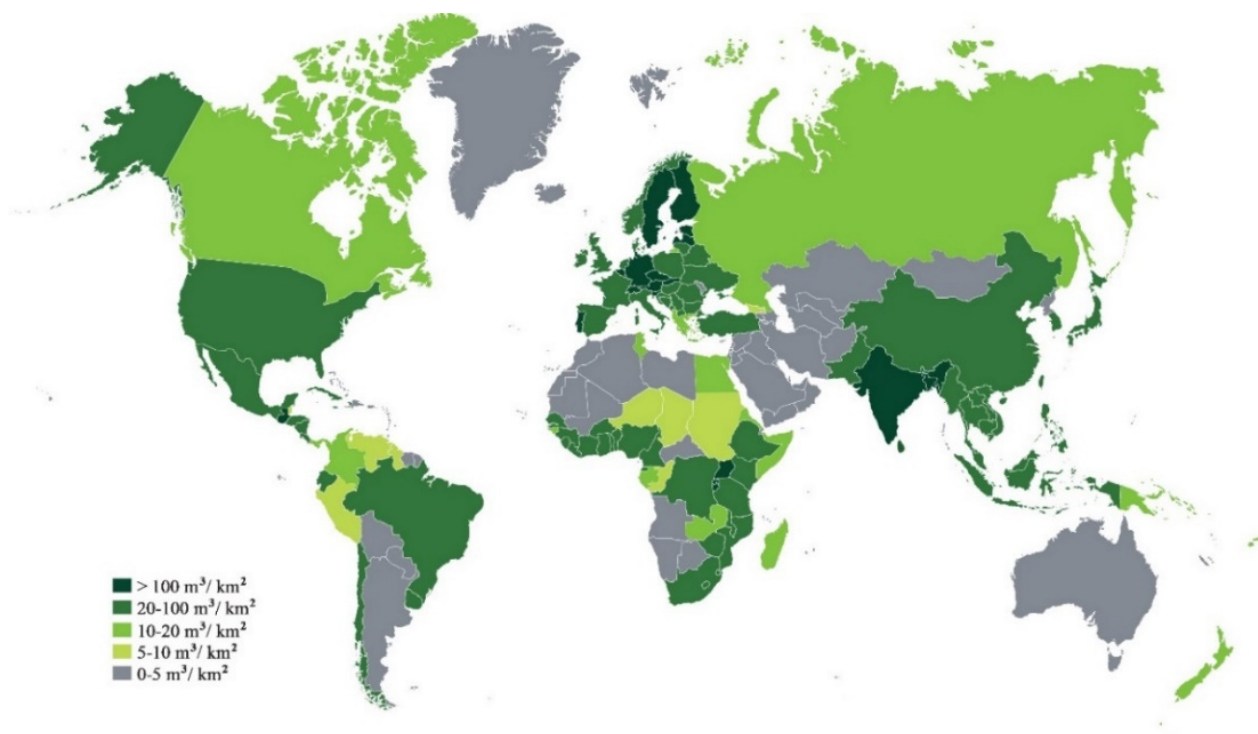


Figure 1. Global wood harvest [1].

Moreover, the investigation of the effect of the fibre length on the properties of unfired clay blocks is also gaining particular attention in the literature. Sangma et al. [36] used various lengths of coconut fibres (20–80 mm) with soil as a reinforcing material and observed that with increasing fibre sizes up to 40 mm, the average compressive strength and splitting tensile strength increased, and thereafter, they decreased. Mostafa and Uddin [37] incorporated 50 to 100 mm banana fibres to manufacture compressed earth blocks, and the findings indicated that the blocks reinforced with 60 mm and 70 mm fibre lengths had the maximum compressive and bending strengths compared to the other samples. Laibi et al. [38] produced compressed earth blocks utilising different kenaf fibre lengths (10, 20 and 30 mm) and evaluated their influence on the mechanical and thermal characteristics of the samples. The results indicated that while the positive effect on the flexural strength was produced by shorter kenaf fibres (10 and 20 mm), the best result was achieved with a fibre length of 30 mm. Additionally, the thermal conductivity values declined gradually with the increase in the fibre length. In another study, the influence of three various pig hair lengths (7 mm, 15 mm and 30 mm) on adobe was investigated by Araya-Letelier et al. [39]. According to the findings, a longer pig hair length resulted in lower average compressive and flexural strength values. This was explained by the clustering of the longer fibres in the mixture which resulted in weak adhesion between the clustered fibres and the earthen matrix. Moreover, the drying shrinkage decreased for higher percentages and longer fibre lengths. Millogo et al. [40] found that using shorter kenaf fibres (30 mm) reduced the pore size and improved the compressive strength more than using longer fibres (60 mm) in pressed adobe blocks.

The conclusions drawn from the experimental results provided in the literature are often inconsistent. As a result, additional study is needed to offer comprehensive knowledge on this subject. Therefore, this research aimed to investigate how three distinct sawdust particle sizes affect the physical and mechanical characteristics of unfired clay blocks. The tests included density, linear shrinkage, capillary water absorption, flexural strength (FS) and compressive strength (CS). Three groups of samples: SP-a ($212 \mu\text{m} < x < 300 \mu\text{m}$), SP-b ($425 \mu\text{m} < x < 600 \mu\text{m}$) and SP-c ($1.18 \text{ mm} < x < 2.00 \text{ mm}$), were prepared with different percentages (0.25–10%) of sawdust. The findings of the experiments were analysed and compared with the reference sample to draw useful conclusions about the influence of the particle size and amount on the characteristics of the unfired clay blocks. The results of incorporating different particle sizes of sawdust provide intriguing additional data that would support evaluating the potential use of sawdust in the manufacturing of unfired clay blocks.

2. Materials and Methods

2.1. Raw Materials

The raw materials utilised in this study were red clay powder (RCP) and sawdust powder (SP). Red clay was obtained from Bath Potters' Supplies, and sawdust (softwood-based and homogeneous) was collected from a local retailer in the United Kingdom. The water used was normal tap water at a temperature of $20 \pm 2^\circ\text{C}$. According to the standard proctor test [41], the clay had the optimum moisture content of 15.50% and a maximum dry density of 2320 kg/m^3 . The Atterberg limit of clay was determined following the BS 1377-2:1990 standard [42]. The clay had a plastic limit of 19.25% water content and a liquid limit of 31.61%, indicating that it was a medium plastic clay with a plasticity index of 12.36%. X-ray fluorescence (XRF) and X-ray diffraction (XRD) analyses were performed to analyse the chemical and mineralogical compositions of raw materials. Figure 2 illustrates the XRD analysis. Tables 1 and 2 show the properties of the RCP and SP, respectively. Quartz was identified as the main mineralogical phase in clay by the XRD pattern (Figure 2a). Other mineralogical phases found in the clay were kaolinite ($\text{Al}_2\text{Si}_2\text{O}_5(\text{OH})_4$) and haematite (Fe_2O_3). On the other hand, the sawdust contained amorphous phases such as hemicelluloses and lignin, as evidenced by the disordered nature of the XRD pattern (Figure 2b). The only crystalline phase found was cellulose, which exhibited a sharp peak at 22.6° and

a broad peak between 15° and 18° as well as a wideband peak at 35° . SP-a, SP-b and SP-c had bulk densities of 0.26 g/cm^3 , 0.23 g/cm^3 and 0.20 g/cm^3 and specific gravities of 1.23, 1.14 and 1.02, respectively. It was observed that as the size of the sawdust increased, its density decreased slightly.

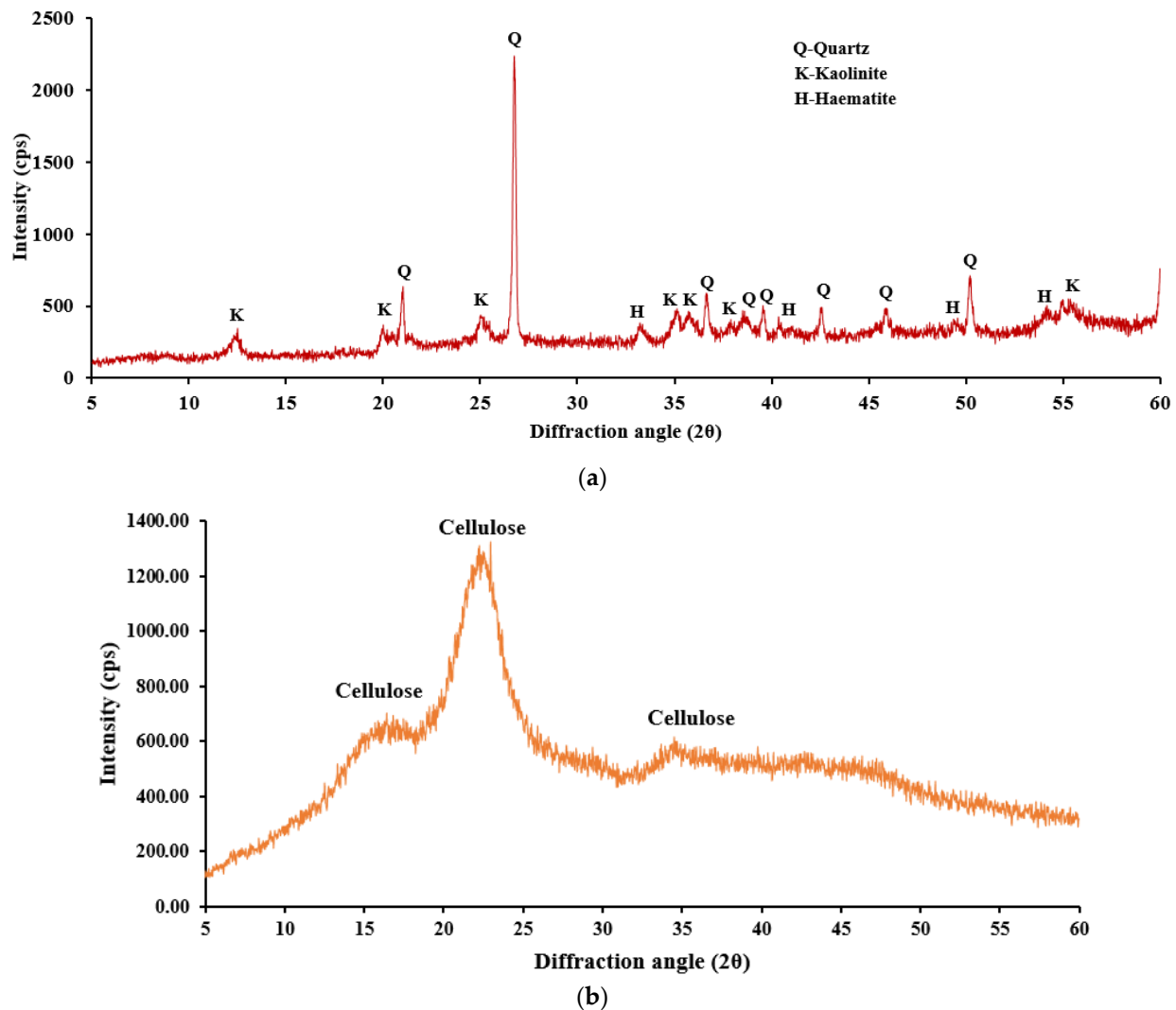


Figure 2. XRD analysis: (a) red clay powder (RCP) (b) sawdust powder (SP).

2.2. Sample Preparation

The RCP was sieved through a 2 mm sieve and stored at the laboratory room temperature until it was formed into clay blocks. The SP was categorised into three particle size ranges: SP-a ($212 \mu\text{m} < x < 300 \mu\text{m}$), SP-b ($425 \mu\text{m} < x < 600 \mu\text{m}$) and SP-c ($1.18 \text{ mm} < x < 2.00 \text{ mm}$) (Figure 3). Two sets of samples were cast, one simply using clay (Reference block), and the other using SP as an additive (Composite blocks). The samples with SP were grouped into three particle size distributions (SP-a, SP-b and SP-c). For each particle size group, samples were produced with the percentage of the additives ranging from 2.5 to 10% of the dry wt of clay. The amounts of raw materials stated in Table 3 were first blended thoroughly in the dry state in a mechanical mixer. Then, the mixture was further thoroughly combined with sufficient water to achieve a workable consistency for moulding. The mixture was placed in steel moulds in two layers and hand compacted. The size of the raw clay blocks used in the testing was determined according to the EN 1015-11 standard [43], which is a $40 \times 40 \times 160 \text{ mm}$ prism (Figure 4). The samples were covered

with plastic sheets for a week before being removed from the moulds and then allowed to cure for 21 days at the laboratory room temperature of 23–26 °C and relative humidity of 30–34% prior to testing.

Table 1. Properties of the red clay powder (RCP).

Optimum moisture content	15.50%
Maximum dry density (kg/m ³)	2320
Liquid limit (%)	31.61
Plastic limit (%)	19.25
Plasticity index (%)	12.36
Bulk density (g/cm ³)	1.43
Specific gravity	2.32
Natural moisture content (%)	6.47
Colour	Red
Chemical Compounds (%)	
SiO ₂	41.454
Al ₂ O ₃	15.214
Fe ₂ O ₃	8.104
MgO	5.114
K ₂ O	1.636
TiO ₂	1.411
Na ₂ O	1.027
CaO	0.633
BaO	0.216
SO ₃	0.047
MnO	0.040

Table 2. Properties of the sawdust powder (SP).

Items				SP-a		SP-b		SP-c		
Particle Size				212 μm < x < 300 μm		425 μm < x < 600 μm		1.18 mm < x < 2.00 mm		
Bulk density (g/cm ³)				0.26		0.23		0.20		
Specific gravity				1.23		1.14		1.02		
Natural moisture content (%)						5.02				
Colour						Light brown				
Chemical Compounds (%)										
SiO ₂	Al ₂ O ₃	Fe ₂ O ₃	MgO	K ₂ O	TiO ₂	Na ₂ O	CaO	BaO	SO ₃	MnO
0.348	0.390	0.186	0.408	0.340	0.171	0.926	1.681	0.074	0.049	0.026



Figure 3. Raw materials: (a) RCP; (b) SP-a; (c) SP-b; (d) SP-c.

Table 3. Mix ID and material proportions.

Mix ID	Clay (g)	SP (%)	SP (g)
R (Reference)	550	0	0
Group A			
S-a-2.5	550	2.5	13.75
S-a-5	550	5	27.50
S-a-7.5	550	7.5	41.25
S-a-10	550	10	55
Group B			
S-b-2.5	550	2.5	13.75
S-b-5	550	5	27.50
S-b-7.5	550	7.5	41.25
S-b-10	550	10	55
Group C			
S-c-2.5	550	2.5	13.75
S-c-5	550	5	27.50
S-c-7.5	550	7.5	41.25
S-c-10	550	10	55



Figure 4. Three groups of prism samples.

2.3. Experimental Tests

All the physical and mechanical property tests of the produced clay blocks were performed after 28 days of the drying period. The average of three samples was used to calculate the results of all tests.

2.3.1. Physical Property Tests

XRD analyses were performed to identify the crystal structure in the composites. For the XRD test, finely ground powder from the samples after 28 days of the drying period was used. The analysis was conducted using a Rigaku mini-flex XRD analyser (30 kV voltage and 15 mA) with Cu K radiation. The data were collected at an angular speed of 2°/min in continuous scan mode for a 2θ angle from 5° to 60°.

The densities of the samples were calculated by dividing the dry weight of the samples by their volume. The volume was obtained by taking measurements of the sample in all three dimensions with digital callipers.

BS EN 1015-18 [44] specifies the test procedure of the capillarity water absorption coefficient. The half prism samples from the flexural strength were employed for the test. In accordance with the standard, the half prisms were oven dried at 60 ± 5 °C for 24 h in a ventilated oven to attain constant mass, and the oven-dried masses were recorded. The

samples were then placed on their bases in a container of 5 mm-deep water and weighed again after 10 min (Figure 5a). The capillarity water absorption coefficient was determined using the following Equation (1) [44]:

$$C_w = 0.1 \times (M_t - M_i) \quad (1)$$

where C_w ($\text{kg}/(\text{m}^2 \cdot \text{min}^{0.5})$) is the capillarity water absorption coefficient, M_t (kg) is the weight of the sample removed from the water after 10 min, and M_i (kg) is the weight of the oven-dried sample.

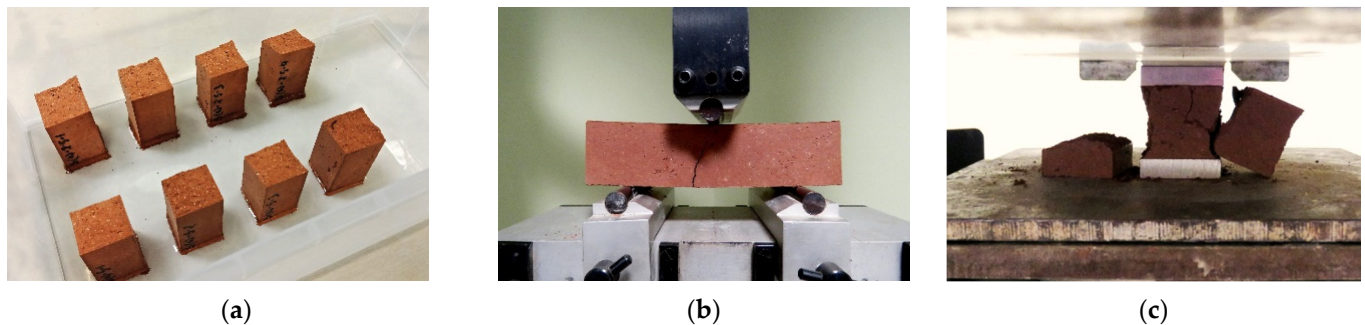


Figure 5. Experimental tests: (a) capillary water absorption; (b) flexural strength; (c) compressive strength.

Linear shrinkages of the samples were determined by measuring the initial length of the samples after casting and the length after the drying period with a digital calliper. They are expressed as the percentage of the ratio of the difference in drying length to the initial length.

2.3.2. Mechanical Property Tests

The flexural strength test was carried out on the full prism samples ($40 \times 40 \times 160$ mm) according to the 3-point bending test described in EN 1015-11 [43] (Figure 5b). The load was applied to the samples at a rate of 10 N/s until the failure occurred. The flexural strength (f , MPa) was calculated using Equation (2):

$$f = \frac{1.5FL}{bd^2} \quad (2)$$

where F (N) is the rupture load, L (mm) is the distance between the supports, d (mm) is the width of the sample, and b (mm) is its height.

After breaking each prism sample in the flexural strength test according to EN 1015-11, half prism samples were tested for compressive strength. Both air-dried and oven-dried (60 ± 5 °C for 24 h) samples were tested for compressive strength. The samples were sandwiched between two bearing steel plates (Figure 5c) and compressed at a rate of 0.40 MPa/s until observable damage resulted from the compression. The compressive strength (C , MPa) was determined using the maximum sustained load (F , kN) and the surface area (A , mm^2) of the samples on which the load was applied:

$$C = \frac{F}{A} \quad (3)$$

3. Results and Discussions

3.1. Physical Properties

The XRD result (Figure 6) shows that the addition of SP did not lead to the formation of new mineral phases.

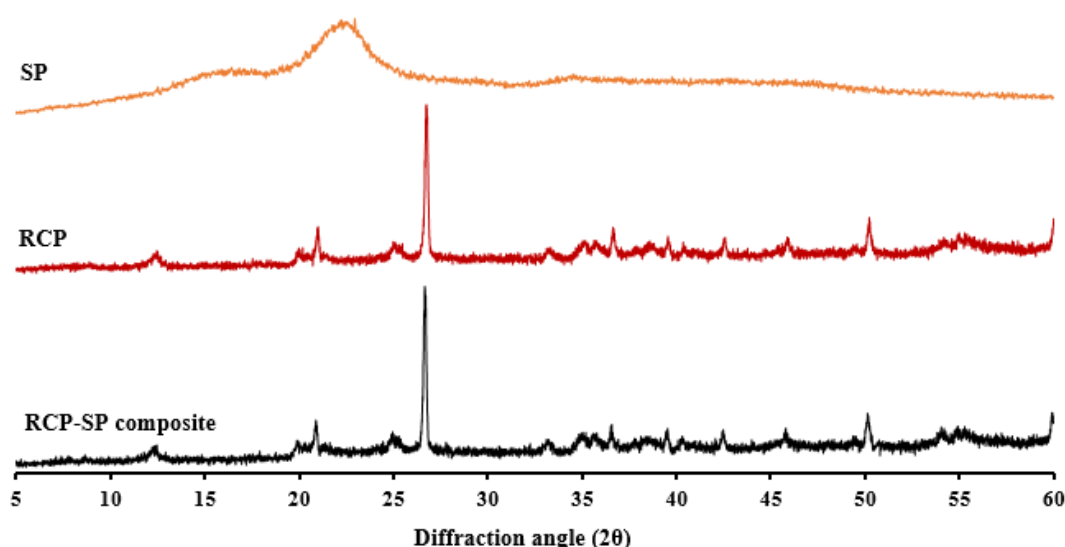


Figure 6. XRD analysis of SP-incorporated sample.

3.1.1. Density

From Figure 7, it can be observed that for all three groups, samples containing 2.5% sawdust had densities of $\geq 1750 \text{ kg/m}^3$, which fulfilled the criteria of the IS 1725 and SLS 1382 standards [45,46]; therefore, they can be used as load-bearing units according to the standards. Additionally, the sample with 5% SP-a met the standard criteria, with a density of 1776 kg/m^3 . In general, the samples with the lowest sawdust percentage had the highest densities, and for all three groups, densities decreased as the sawdust amount increased in the mixture. Several researchers noticed a similar trend when they combined lignocellulosic fibres with earth [47–54]. With the same percentages of the SP content, SP-a-blended samples had slightly higher densities compared to the other two groups. This is in line with the fact that SP-a had a higher specific gravity (1.23) than SP-b (1.14) and SP-c (1.02). This can also be explained by the particle size difference of each group. SP-c had a larger particle size, resulting in more gaps between the SP and the clay matrix, but SP-a had considerably smaller particle dimensions, resulting in a more homogenous end product, with fewer pores and a higher density. The densities of the samples decreased from 1861 to 1611 kg/m^3 (SP-a), 1837 to 1476 kg/m^3 (SP-b) and 1781 to 1422 kg/m^3 (SP-c) with 2.5% to 10% sawdust addition, corresponding to around 23%, 29% and 32% decreases compared to the reference sample (2091 kg/m^3).

3.1.2. Capillary Water Absorption

The water absorption value can indicate the porosity of the matrix, with a higher water absorption value indicating a higher porosity. Moreover, the open porosity of the samples determines how much water may be absorbed by the capillary. In this study, it was observed that the capillary water absorption coefficient increased as the amount of SP increased in the three groups of samples (Figure 8). The capillary water absorption was higher for SP-a samples than the other two groups. The increase was up to around 34%, 27% and 25% for SP-a, SP-b and SP-c, respectively, compared to the reference sample. This might be related to the pore structure of the samples which is caused by the particle size of the sawdust. Capillary water absorption is inversely proportional to the diameter of the pores, where the smaller the diameter, the greater the capillary absorption [55–57]. When sawdust with larger particle dimensions was used to make clay blocks, it typically resulted in a more porous microstructure with pores of larger diameters. Sawdust with smaller particle dimensions, on the other hand, resulted in better compaction and therefore the formation of finer pores, and finer pores absorb water faster because of the increased capillary pressures produced by them [35,58]. Other investigations on lignocellulosic fibre-

earth composites found similar results, indicating that larger percentages of fibre resulted in higher absorption levels [49,59–61]. In addition, the results indicate that capillary water absorption is inversely related to the sample density, with a lower density indicating more porosity and greater capillary water absorption (Figure 9).

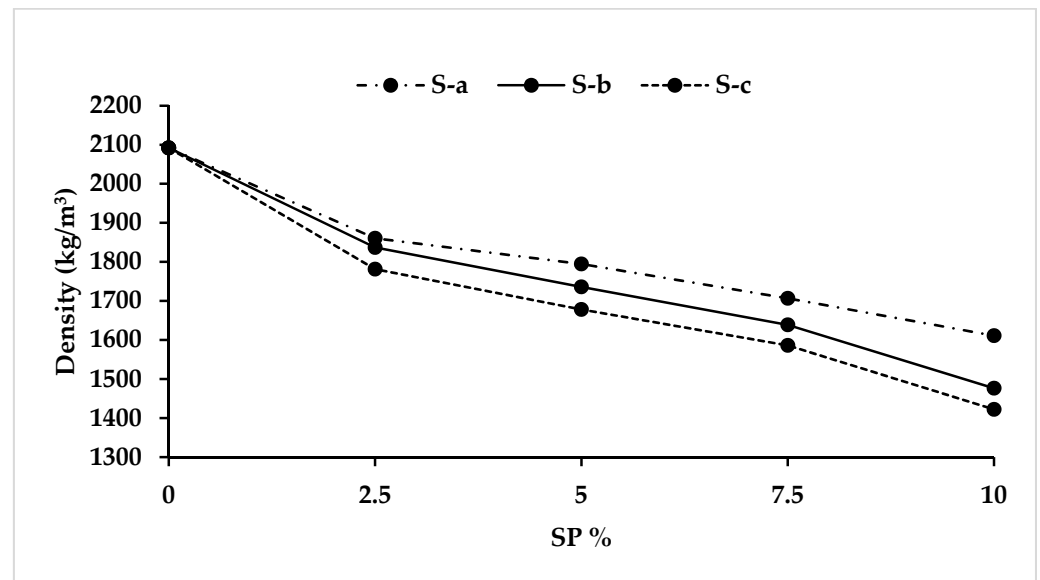


Figure 7. Density results of SP-incorporated samples.

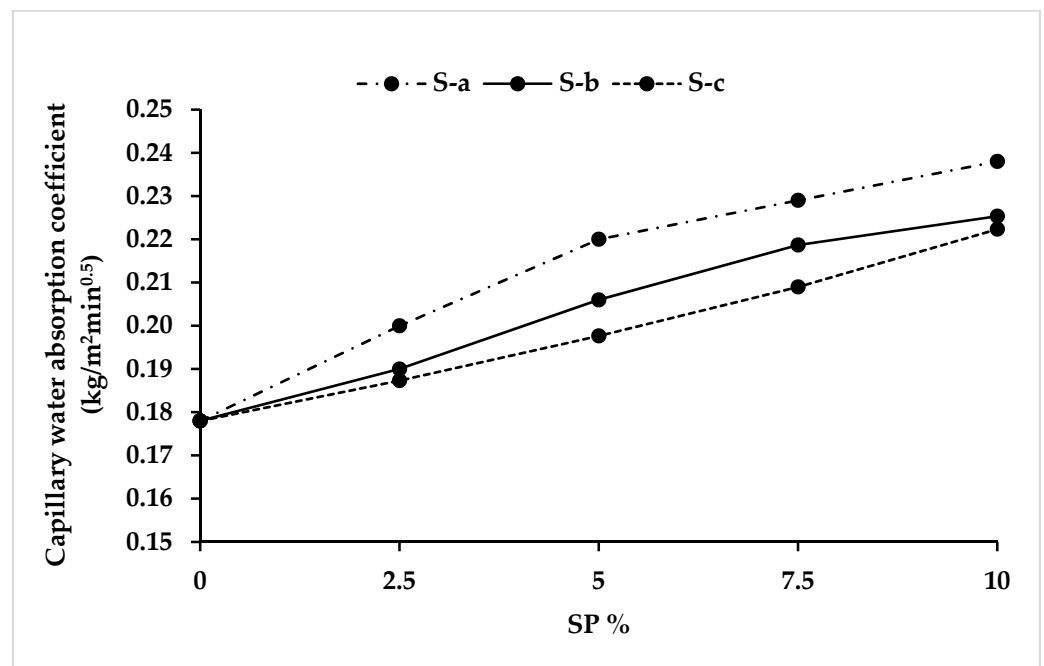


Figure 8. Capillary water absorption coefficient results of SP-incorporated samples.

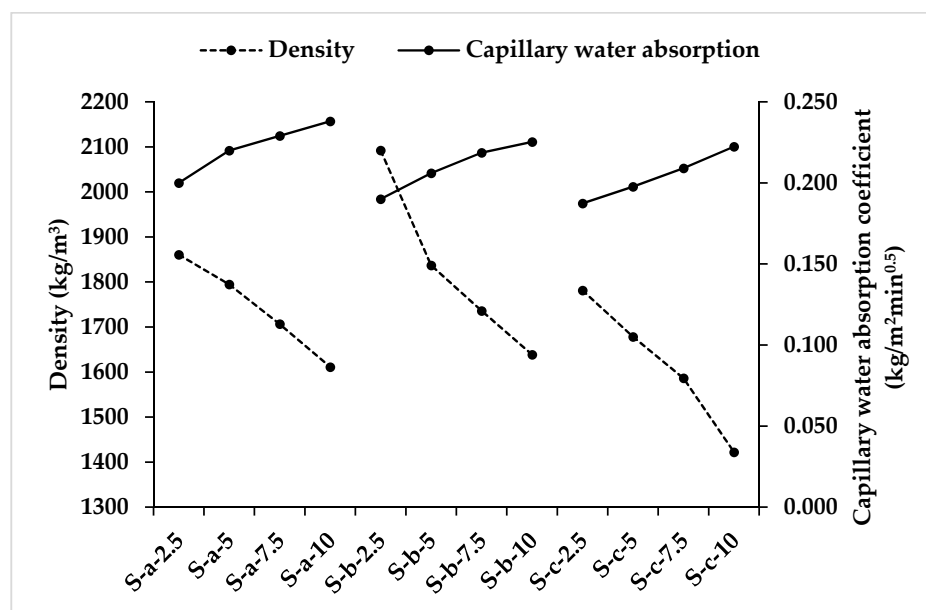


Figure 9. Relation between density and capillary water absorption.

3.1.3. Linear Shrinkage

The linear shrinkage results indicate that by increasing SP-b and SP-c in the mixture, the shrinkage of the samples gradually decreased (Figure 10). The SP-c samples with a larger particle size had a greater linear shrinkage reduction of around 45% (10% SP-c), whereas SP-b (10%) samples had a shrinkage reduction of 31% compared to the reference sample. This is consistent with previous studies [28,49,62,63] which indicated that adding natural fibres to the mixture improved shrinkage. Bouhicha et al. [62] and Araya-Letelier et al. [39] observed that increasing the percentage and length of barley straw and pig hair, respectively, reduced the drying shrinkage of the samples. This could be due to the fibres being long enough for the development of bond stresses at the fibre-soil interface, therefore opposing soil deformation and contraction. On the other hand, in the case of SP-a, the 2.5% content had lower linear shrinkage than the reference sample, but linear shrinkage increased with increasing SP-a content. This result might be explained by the fact that the fibre length is insufficient for the bond stresses to build; however, additional research is required to confirm this.

3.2. Mechanical Properties

Flexural Strength and Compressive Strength

Table 4 summarises the results obtained from the mechanical property tests. The results represent the arithmetic mean of three samples. From Table 4, it is observed that the results of both air-dried and oven-dried samples met the standard requirement of compressive strength (1–2.08 MPa) [45,64–66]. Additionally, the samples fulfilled the flexural strength requirement of the standards (0.25–0.50 MPa) [46,65,66] of unfired earth blocks. The highest compressive and flexural strengths were achieved with the lowest percentage of sawdust content for all groups. It should also be noted that an increase in the content of sawdust led to a decrease in both the compressive and flexural strengths, irrespective of the particle size dimension. Moreover, the best mechanical strength was obtained for SP-b (FS—2.00 MPa, CS—4.74 MPa). It can be observed that the compressive strength trend for oven-dried samples was similar to that of air-dried samples, although oven-dried samples exhibited a higher compressive strength level. Several studies found a similar trend where the strength decreased as the fibre amount increased [35,47,54,61,63]. Moreover, the study of Mostafa and Uddin [37] demonstrated that the strength of compressed earth blocks gradually increased for 50–70 mm banana fibres and then decreased for the

higher lengths of fibres (80–100 mm). As already highlighted by the authors, the decrease in strength depends on the decline in the bulk density, non-homogenous fibre distribution, larger gaps produced by larger fibre lengths and decreased cohesion and bonding between the fibres and the soil matrix of the final products. In Figures 11 and 12, the percentage increase/decrease in the flexural and compressive strengths compared to the reference sample is plotted against different percentages of three types of SP. Figure 11 demonstrates that for the 2.5% content of all three groups, the percentage increase in flexural strength is at a maximum, and above 2.5%, it shows a decreasing trend in the strength increment. However, the flexural strength of SP-a, SP-b and SP-c at 7.5%, 10% and 5% contents, respectively, was lower than the reference sample. As shown in Figure 12, at a 2.5% content, SP-b significantly improved the compressive strength compared to the reference sample, while SP-a marginally enhanced it, and SP-c did not improve it. Moreover, Figures 13 and 14 show that the compressive strength decreased with the decreasing density and increasing capillary water absorption of the samples.

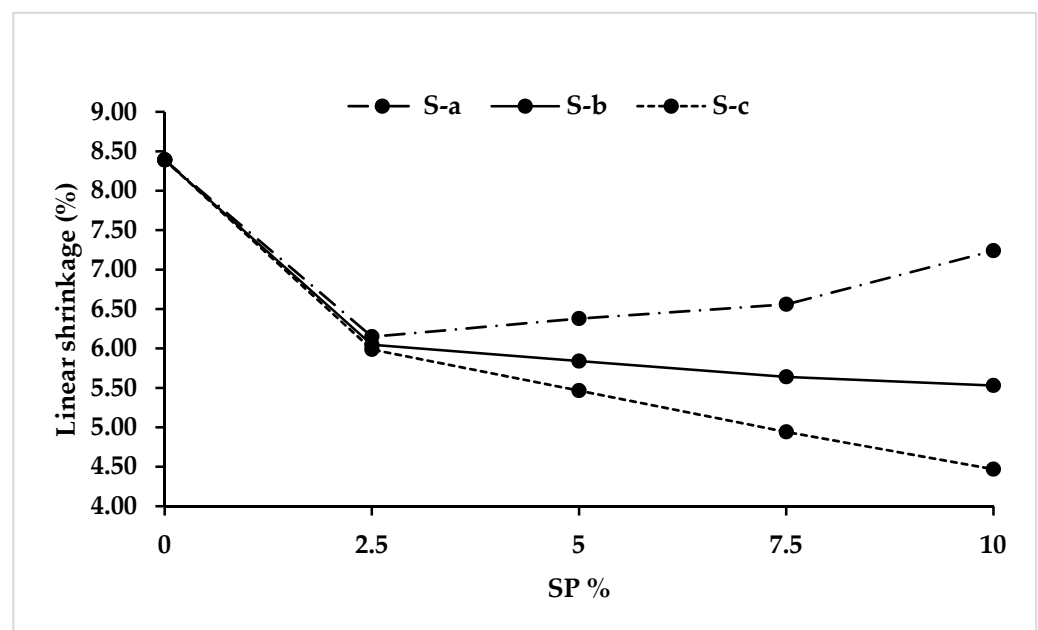


Figure 10. Linear shrinkage results of SP-incorporated samples.

Table 4. Average values and standard deviation (in parenthesis) of mechanical property test results of the stabilised clay blocks.

Mix ID	Flexural Strength (FS)	Compressive Strength (CS) (Air Dried)	Compressive Strength (CS) (Oven Dried)
	Avg. FS (MPa)	Avg. CS (MPa)	Avg. CS (MPa)
R	1.52 (0.14)	4.06 (0.39)	5.40 (0.09)
S-a-2.5	1.69 (0.04)	4.09 (0.06)	5.44 (0.10)
S-a-5	1.57 (0.02)	3.81 (0.05)	5.03 (0.09)
S-a-7.5	1.46 (0.03)	3.55 (0.04)	4.95 (0.27)
S-a-10	1.26 (0.07)	3.33 (0.16)	4.58 (0.05)
S-b-2.5	2.00 (0.03)	4.74 (0.18)	6.28 (0.05)
S-b-5	1.86 (0.04)	4.29 (0.04)	5.82 (0.17)
S-b-7.5	1.65 (0.03)	4.15 (0.03)	5.58 (0.23)
S-b-10	1.36 (0.04)	3.53 (0.09)	4.74 (0.29)
S-c-2.5	1.63 (0.06)	3.90 (0.28)	5.23 (0.04)
S-c-5	1.45 (0.04)	3.45 (0.04)	4.68 (0.08)
S-c-7.5	1.28 (0.01)	3.28 (0.03)	4.35 (0.20)
S-c-10	1.05 (0.06)	3.17 (0.09)	4.19 (0.25)

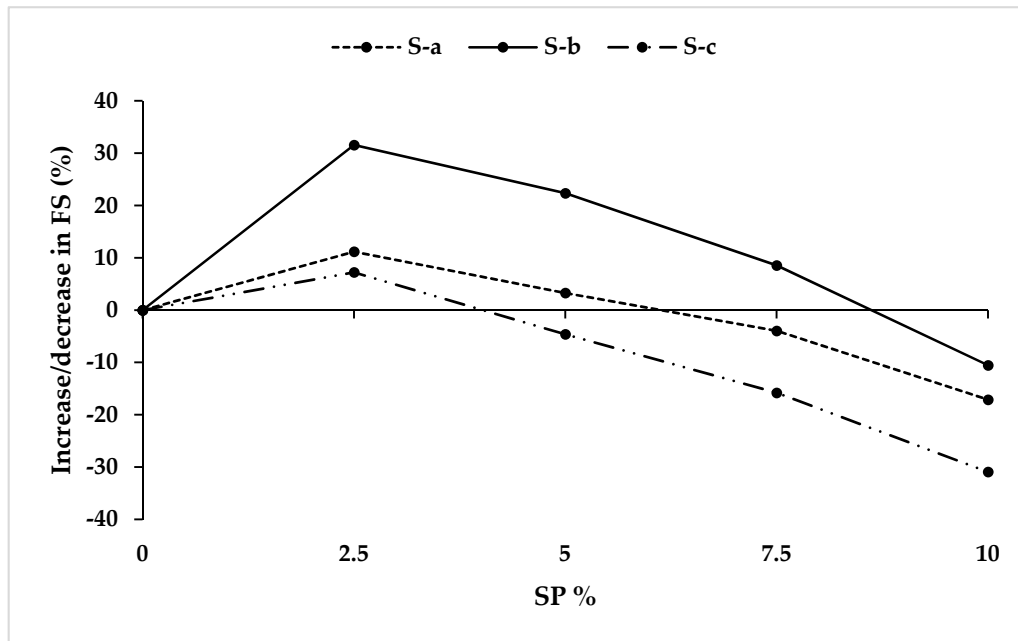


Figure 11. Percentage increase/decrease in flexural strength with increasing SP content.

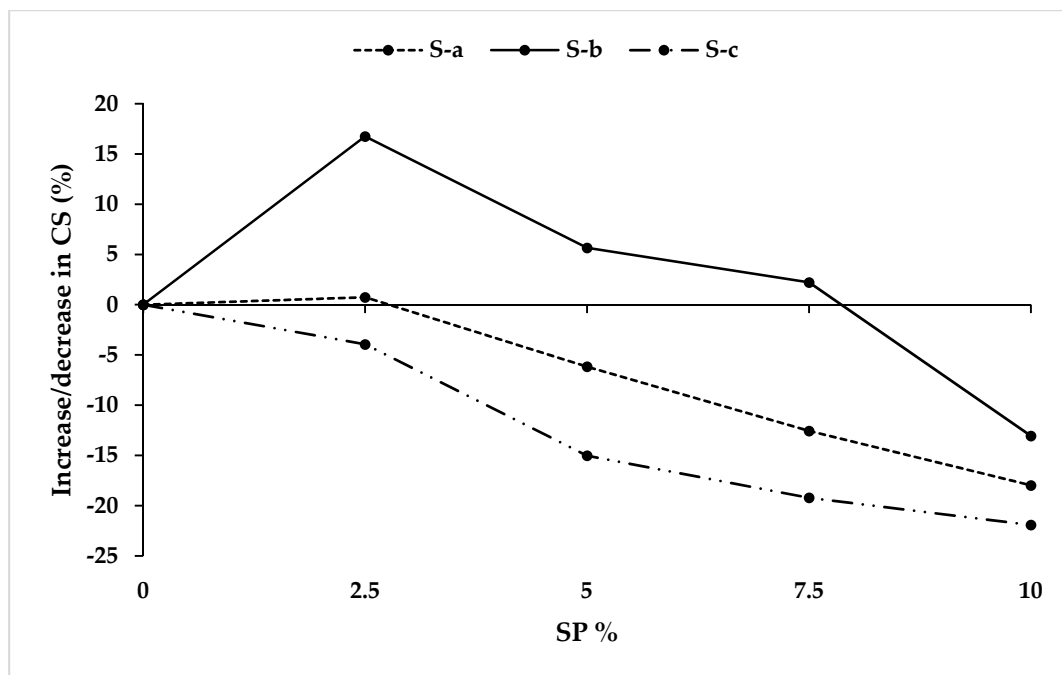


Figure 12. Percentage increase/decrease in compressive strength with increasing SP content.

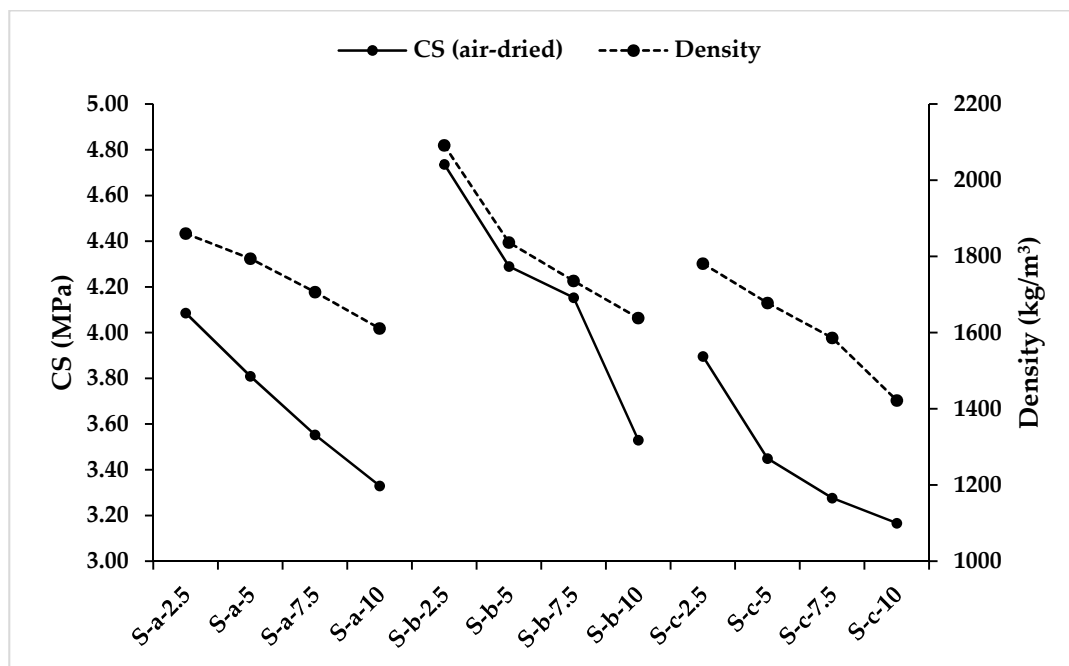


Figure 13. Relation between density and compressive strength.

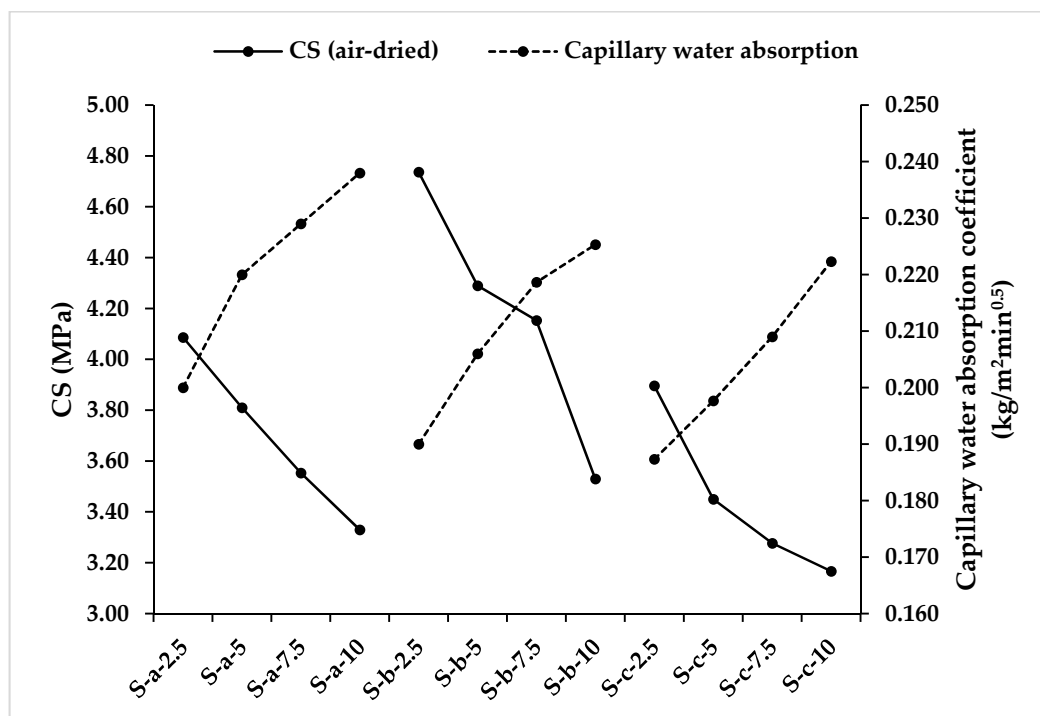


Figure 14. Relation between compressive strength and capillary water absorption.

4. Conclusions

The following conclusions can be derived from the experimental investigation presented in this paper:

- The different particle sizes of SP had influences on the physical and mechanical properties of the SP-blended clay blocks.

- The SP inclusion decreased the density of the samples compared to the reference sample due to its lower specific gravity. SP-c samples were lower in density than the other two groups of samples.
- In comparison to the reference sample, the linear shrinkage of the three groups of samples reduced when SP was added to the mixture. However, by increasing the finer particle size of the sawdust (SP-a), linear shrinkage increased, while larger particle (SP-b and SP-c) additions decreased the linear shrinkage values.
- The capillary water absorption coefficient values increased for all groups as the percentage of SP increased, and the values were higher than the reference sample. The increase was higher for the SP-a group compared to the other groups.
- All the SP-incorporated clay blocks fulfilled the strength requirements of the standard for unfired earthen blocks, and the highest strength was achieved at 2.5% of SP content. SP-a and SP-b improved the compressive strength of the samples compared to the reference sample. However, SP-c did not improve the compressive strength. Moreover, the flexural strength showed a similar trend to the compressive strength. Moreover, SP-b (600–425 µm) had a higher strength than the other groups at the same percentage of content.
- The sawdust content of 2.5% with particle sizes ranging between 600 and 425 µm can be utilised to manufacture good-quality unfired clay blocks as it showed the highest mechanical strength and improved the physical properties compared to the other mix proportions and particle sizes.

Further study on the thermal and durability characteristics of different particle size SP-incorporated clay blocks might be an intriguing way to complete the assessment of the potential benefits of the utilisation of SP in the production of unfired clay blocks.

Author Contributions: Methodology, N.J. and R.L.A.-M.; investigation, N.J.; supervision, R.L.A.-M.; writing—original draft, N.J., R.L.A.-M. and A.H.; writing—review and editing, A.H., B.A. and A.C. All authors have read and agreed to the published version of the manuscript.

Funding: This research received no external funding.

Acknowledgments: The authors acknowledge the financial and laboratory support provided by the School of Civil Engineering and Built Environment at Liverpool John Moores University, UK.

Conflicts of Interest: The authors declare no conflict of interest.

References

1. Kirilenko, A.P.; Sedjo, R.A. Climate change impacts on forestry. *Proc. Natl. Acad. Sci. USA* **2007**, *104*, 19697–19702. [CrossRef] [PubMed]
2. FAO. FAOSTAT Data. Available online: <http://www.fao.org/state-of-forests> (accessed on 12 April 2021).
3. Zhang, Q.; Li, Y.; Yu, C.; Qi, J.; Yang, C.; Cheng, B.; Liang, S. Global timber harvest footprints of nations and virtual timber trade flows. *J. Clean. Prod.* **2020**, *250*, 119503. [CrossRef]
4. Penna, I. *Understanding the FAO's Wood Supply from Planted Forests Projections*, 1st ed.; Centre for Environmental Management, University of Ballarat: Ballarat, Australia, 2010; Volume 2010.
5. Rominiyi, O.L.; Adaramola, B.A.; Ikumapayi, O.M.; Oginni, O.T.; Akinola, S.A. Potential Utilization of Sawdust in Energy, Manufacturing and Agricultural Industry; Waste to Wealth. *World J. Eng. Technol.* **2017**, *5*, 526–539. [CrossRef]
6. Charis, G.; Danha, G.; Muzenda, E. A review of timber waste utilization: Challenges and opportunities in Zimbabwe. *Procedia Manuf.* **2019**, *35*, 419–429. [CrossRef]
7. Lopez, Y.M.; Paes, J.B.; Gustave, D.; Gonçalves, F.G.; Méndez, F.C.; Nantet, A.C.T. Production of wood-plastic composites using cedrela odorata sawdust waste and recycled thermoplastics mixture from post-consumer products—A sustainable approach for cleaner production in Cuba. *J. Clean. Prod.* **2020**, *244*, 118723. [CrossRef]
8. Pettersen, R.C. The chemical composition of wood. In *The Chemistry of Solid Wood*; ACS Publications: Washington, DC, USA, 1984; Volume 206, pp. 57–126.
9. Horisawa, S.; Sunagawa, M.; Tamai, Y.; Matsuoka, Y.; Miura, T.; Terazawa, M. Biodegradation of nonlignocellulosic substances II: Physical and chemical properties of sawdust before and after use as artificial soil. *J. Wood Sci.* **1999**, *45*, 492–497. [CrossRef]
10. Lachowicz, H.; Wróblewska, H.; Wojtan, R.; Sajdak, M. The effect of tree age on the chemical composition of the wood of silver birch (*Betula pendula* Roth.) in Poland. *Wood Sci. Technol.* **2019**, *53*, 1135–1155. [CrossRef]

11. Mwango, A.; Kambole, C. Engineering Characteristics and Potential Increased Utilisation of Sawdust Composites in Construction—A Review. *J. Build. Constr. Plan. Res.* **2019**, *7*, 59–88. [\[CrossRef\]](#)
12. Zou, S.; Li, H.; Wang, S.; Jiang, R.; Zou, J.; Zhang, X.; Liu, L.; Zhang, G. Experimental research on an innovative sawdust biomass-based insulation material for buildings. *J. Clean. Prod.* **2020**, *260*, 121029. [\[CrossRef\]](#)
13. Akinyemi, A.B.; Afolayan, J.O.; Oluwatobi, E.O. Some properties of composite corn cob and sawdust particle boards. *Constr. Build. Mater.* **2016**, *127*, 436–441. [\[CrossRef\]](#)
14. Savov, V.; Mihajlova, J.; Grigorov, R. Selected physical and mechanical properties of combined wood based panels from wood fibers and sawdust. *Innov. Woodwork. Ind. Eng. Des.* **2019**, *2*, 42–48.
15. Mirski, R.; Dukarska, D.; Derkowski, A.; Czarnecki, R.; Dziurka, D. By-products of sawmill industry as raw materials for manufacture of chip-sawdust boards. *J. Build. Eng.* **2020**, *32*, 101460. [\[CrossRef\]](#)
16. Mirski, R.; Derkowski, A.; Dziurka, D.; Wieruszewski, M.; Dukarska, D. Effects of chip type on the properties of chip-sawdust boards glued with polymeric diphenyl methane diisocyanate. *Materials* **2020**, *13*, 1329. [\[CrossRef\]](#) [\[PubMed\]](#)
17. Orelma, H.; Tanaka, A.; Vuoriluoto, M.; Khakalo, A.; Korpela, A. Manufacture of all-wood sawdust-based particle board using ionic liquid-facilitated fusion process. *Wood Sci. Technol.* **2021**, *55*, 331–349. [\[CrossRef\]](#)
18. Atoyebi, O.D.; Ajamu, S.O.; Odeyemi, S.O.; Ojo, D.J.; Ramonu, J.A.L. *Strength Evaluation of Aluminium Fibre Reinforced Particle Board Made from Sawdust and Waste Glass*; IOP Conference Series: Materials Science and Engineering; IOP Publishing: Bristol, UK, 2021.
19. Mageswari, M.; Vidivelli, B. The use of sawdust ash as fine aggregate replacement in concrete. *J. Environ. Res. Dev.* **2009**, *3*, 720–726.
20. Ghimire, A.; Maharjan, S. Experimental Analysis on the Properties of Concrete Brick With Partial Replacement of Sand by Saw Dust and Partial Replacement of Coarse Aggregate by Expanded Polystyrene. *J. Adv. Coll. Eng. Manag.* **2019**, *5*, 27–36. [\[CrossRef\]](#)
21. Okunade, E.A. The Effect of Wood Ash and Sawdust Admixtures on the Engineering Properties of a Burnt Laterite-Clay Brick. *J. Appl. Sci.* **2008**, *8*, 1042–1048. [\[CrossRef\]](#)
22. Aramide, F.O. Production and characterization of porous insulating fired bricks from Ifon clay with varied sawdust admixture. *J. Miner. Mater. Charact. Eng.* **2012**, *11*, 970–975. [\[CrossRef\]](#)
23. Chemani, B.; Chemani, H. Effect of adding sawdust on mechanical-physical properties of ceramic bricks to obtain lightweight building material. *Int. J. Mech. Aerosp. Ind. Mechatron. Manuf. Eng.* **2012**, *6*, 2521–2525. [\[CrossRef\]](#)
24. Chemani, H.; Chemani, B. Valorization of wood sawdust in making porous clay brick. *Sci. Res. Essays* **2013**, *8*, 609–614.
25. Hassan, M.A.; Yami, A.M.; Raji, A.; Ngala, M.J. Effects of sawdust and rice husk additives on properties of local refractory clay. *Int. J. Eng. Sci.* **2014**, *3*, 40–44. Available online: <http://www.theijes.com/papers/v3-i8/Version-2/E0382040044.pdf> (accessed on 18 May 2021).
26. Cultrone, G.; Aurrekoetxea, I.; Casado, C.; Arizzi, A. Sawdust recycling in the production of lightweight bricks: How the amount of additive and the firing temperature influence the physical properties of the bricks. *Constr. Build. Mater.* **2020**, *235*, 117436. [\[CrossRef\]](#)
27. Demir, I. Effect of organic residues addition on the technological properties of clay bricks. *Waste Manag.* **2008**, *28*, 622–627. [\[CrossRef\]](#) [\[PubMed\]](#)
28. Vilane, B.R.T. Assessment of stabilisation of adobes by confined compression tests. *Biosyst. Eng.* **2010**, *106*, 551–558. [\[CrossRef\]](#)
29. Ganga, G.; Nsongo, T.; Elenga, H.; Mabiala, B.; Tatsiete, T.T. Effect of incorporation of chips and wood dust mahogany on mechanical and acoustic behavior of brick clay. *J. Build. Constr. Plan. Res.* **2014**, *2*, 198–208. [\[CrossRef\]](#)
30. Ouattara, S.; Boffoue, M.O.; Assande, A.A.; Kouadio, K.C.; Kouakou, C.H.; Emeruwa, E.; Pasres. Use of Vegetable Fibers as Reinforcement in the Structure of Compressed Ground Bricks: Influence of Sawdust on the Rheological Properties of Compressed Clay Brick. *Am. J. Mater. Sci. Eng.* **2016**, *4*, 13–19. [\[CrossRef\]](#)
31. Fadele, O.A.; Ata, O. Water absorption properties of sawdust lignin stabilised compressed laterite bricks. *Case Stud. Constr. Mater.* **2018**, *9*, e00187. [\[CrossRef\]](#)
32. Jokhio, G.A.; Mohsin, S.M.S.; Gul, Y. *Two-Fold Sustainability—Adobe with Sawdust as Partial Sand Replacement*; IOP Conference Series: Materials Science and Engineering; IOP Publishing: Bristol, UK, 2018.
33. Ayodele, A.L.; Oketope, O.M.; Olatunde, O.S. Effect of sawdust ash and eggshell ash on selected engineering properties of lateralized bricks for low cost housing. *Niger. J. Technol.* **2019**, *38*, 278–282. [\[CrossRef\]](#)
34. Charai, M.; Sghouri, H.; Mezrhab, A.; Karkri, M.; Elhammouti, K.; Nasri, H. Thermal performance and characterization of a sawdust-clay composite material. *Procedia Manuf.* **2020**, *46*, 690–697. [\[CrossRef\]](#)
35. De Castrillo, M.C.; Ioannou, I.; Philokyprou, M. Reproduction of traditional adobes using varying percentage contents of straw and sawdust. *Constr. Build. Mater.* **2021**, *294*, 123516. [\[CrossRef\]](#)
36. Sangma, S.; Pohti, L.; Tripura, D.D. Size Effect of Fiber on Mechanical Properties of Mud Earth Blocks. In *Recycled Waste Materials*; Springer: Singapore, 2019; pp. 119–125.
37. Mostafa, M.; Uddin, N. Experimental analysis of Compressed Earth Block (CEB) with banana fibers resisting flexural and compression forces. *Case Stud. Constr. Mater.* **2016**, *5*, 53–63. [\[CrossRef\]](#)
38. Laibi, A.B.; Poullain, P.; Leklou, N.; Gomina, M.; Sohounhloué, D.K.C. Influence of the kenaf fiber length on the mechanical and thermal properties of Compressed Earth Blocks (CEB). *KSCE J. Civ. Eng.* **2018**, *22*, 785–793. [\[CrossRef\]](#)

39. Araya-Letelier, G.; Concha-Riedel, J.; Antico, F.C.; Valdés, C.; Cáceres, G. Influence of natural fiber dosage and length on adobe mixes damage-mechanical behavior. *Constr. Build. Mater.* **2018**, *174*, 645–655. [\[CrossRef\]](#)
40. Millogo, Y.; Morel, J.-C.; Aubert, J.-E.; Ghavami, K. Experimental analysis of Pressed Adobe Blocks reinforced with Hibiscus cannabinus fibers. *Constr. Build. Mater.* **2014**, *52*, 71–78. [\[CrossRef\]](#)
41. ASTM D698; *Standard Test Methods for Laboratory Compaction Characteristics of Soil Using Standard Effort (12,400 ft-lbf/ft³ (600 kN-m/m³))*; ASTM International: West Conshohocken, PA, USA, 2012.
42. BS 1377-2; *Methods of Test for Soils for Civil Engineering Purposes, Part 2: Classification Tests*; British Standards Institution: London, UK, 1990.
43. BS EN 1015-11; *Methods of Test for Mortar for Masonry. Part 11: Determination of Flexural and Compressive Strength of Hardened Mortar*; British Standards Institution: London, UK, 2019.
44. BS EN 1015-18; *Methods of Test for Mortar for Masonry, Part 18: Determination of Water Absorption Coefficient due to Capillary Action of Hardened Mortar*; British Standards Institution: London, UK, 2002.
45. SLS 1382; *Specification for Compressed Stabilized Earth Blocks*; Sri Lanka Standards Institution: Colombo, Sri Lanka, 2009.
46. IS: 1725; *Specification for Soil Based Blocks Used in General Building Construction*; Bureau of Indian Standards: New Delhi, India, 1982.
47. Khedari, J.; Watsanasathaporn, P.; Hirunlabh, J. Development of fibre-based soil–cement block with low thermal conductivity. *Cem. Concr. Compos.* **2005**, *27*, 111–116. [\[CrossRef\]](#)
48. Ashour, T.; Korjenic, A.; Korjenic, S.; Wu, W. Thermal conductivity of unfired earth bricks reinforced by agricultural wastes with cement and gypsum. *Energy Build.* **2015**, *104*, 139–146. [\[CrossRef\]](#)
49. Danso, H.; Martinson, D.B.; Ali, M.; Williams, J.B. Physical, mechanical and durability properties of soil building blocks reinforced with natural fibres. *Constr. Build. Mater.* **2015**, *101*, 797–809. [\[CrossRef\]](#)
50. Zak, P.; Ashour, T.; Korjenic, A.; Korjenic, S.; Wu, W. The influence of natural reinforcement fibers, gypsum and cement on compressive strength of earth bricks materials. *Constr. Build. Mater.* **2016**, *106*, 179–188. [\[CrossRef\]](#)
51. Laborel-Préneron, A.; Aubert, J.-E.; Magniont, C.; Maillard, P.; Poirier, C. Effect of plant aggregates on mechanical properties of earth bricks. *J. Mater. Civ. Eng.* **2017**, *29*, 04017244. [\[CrossRef\]](#)
52. Giroudon, M.; Laborel-Préneron, A.; Aubert, J.-E.; Magniont, C. Comparison of barley and lavender straws as bioaggregates in earth bricks. *Constr. Build. Mater.* **2019**, *202*, 254–265. [\[CrossRef\]](#)
53. Ojo, E.B.; Bello, K.O.; Mustapha, K.; Teixeira, R.S.; Santos, S.F.; Savastano, H., Jr. Effects of fibre reinforcements on properties of extruded alkali activated earthen building materials. *Constr. Build. Mater.* **2019**, *227*, 116778. [\[CrossRef\]](#)
54. Wang, Z.; Zhao, C.; Zhang, Y.; Hua, B.; Lu, X. *Study on Strength Characteristics of Straw (EPS Particles)-Sparse Sludge Unburned Brick*; IOP Conference Series: Materials Science and Engineering; IOP Publishing: Bristol, UK, 2019.
55. Borrelli, E. *Conservation of Architectural Heritage, Historic Structures and Materials*; ICCROM: Rome, Italy, 1990; Volume 2.
56. Harries, K.A.; Sharma, B. *Nonconventional and Vernacular Construction Materials: Characterisation, Properties and Applications*; Woodhead Publishing: Cambridge, UK, 2019.
57. Kim, M.; Kang, S.-H.; Hong, S.-G.; Moon, J. Influence of effective water-to-cement ratios on internal damage and salt scaling of concrete with superabsorbent polymer. *Materials* **2019**, *12*, 3863. [\[CrossRef\]](#)
58. Hall, C.; Hoff, W.D. Water Transport. In *Brick, Stone and Concrete*, 2nd ed.; CRC Press, Taylor & Francis Group: Boca Raton, FL, USA, 2002.
59. Taallah, B.; Guettala, A.; Guettala, S.; Kriker, A. Mechanical properties and hygroscopicity behavior of compressed earth block filled by date palm fibers. *Constr. Build. Mater.* **2014**, *59*, 161–168. [\[CrossRef\]](#)
60. Ouedraogo, M.; Dao, K.; Millogo, Y.; Aubert, J.-E.; Messan, A.; Seynou, M.; Zerbo, L.; Gomina, M. Physical, thermal and mechanical properties of adobes stabilized with fonio (*Digitaria exilis*) straw. *J. Build. Eng.* **2019**, *23*, 250–258. [\[CrossRef\]](#)
61. Thanushan, K.; Yogananth, Y.; Sangeeth, P.; Coonghe, J.G.; Sathiparan, N. Strength and durability characteristics of coconut fibre reinforced earth cement blocks. *J. Nat. Fibers* **2019**, *18*, 773–788. [\[CrossRef\]](#)
62. Bouhicha, M.; Aouissi, F.; Kenai, S. Performance of composite soil reinforced with barley straw. *Cem. Concr. Compos.* **2005**, *27*, 617–621. [\[CrossRef\]](#)
63. Murillo, C.G.; Walker, P.J.; Ansell, M.P. Henequen Fibres for Reinforcement of Unfired Earth Blocks. In *Proceedings of the Eleventh International Conference for Renewable Resources and Plant Biotechnology (NAROSSA)*, Poznan, Poland, 6–7 June 2005.
64. TS 2514. *Adobe Blocks and Production Methods*; Turkish Standards Institute: Ankara, Turkey, 1977. (In Turkish)
65. CID-GCBNMBC-91-1; *New Mexico Adobe and Rammed Earth Building Code*; General Construction Bureau, Regulation & Licensing Department: Santa Fe, NM, USA, 1991.
66. NZS 4298. *Materials and Workmanship of Earth Buildings*; Standard New Zealand: Wellington, New Zealand, 1998.